



Article scientifique

Article

2007

Published version

Open Access

This is the published version of the publication, made available in accordance with the publisher's policy.

Concordant ages for the giant Kipushi base metal deposit (DR Congo)
from direct Rb–Sr and Re–Os dating of sulfides

Schneider, Jens; Melcher, Frank; Brauns, Michael

How to cite

SCHNEIDER, Jens, MELCHER, Frank, BRAUNS, Michael. Concordant ages for the giant Kipushi base metal deposit (DR Congo) from direct Rb–Sr and Re–Os dating of sulfides. In: Mineralium Deposita, 2007, vol. 42, n° 7, p. 791–797. doi: 10.1007/s00126-007-0158-y

This publication URL: <https://archive-ouverte.unige.ch/unige:116058>

Publication DOI: [10.1007/s00126-007-0158-y](https://doi.org/10.1007/s00126-007-0158-y)

Concordant ages for the giant Kipushi base metal deposit (DR Congo) from direct Rb–Sr and Re–Os dating of sulfides

Jens Schneider · Frank Melcher · Michael Brauns

Received: 30 May 2007 / Accepted: 27 June 2007 / Published online: 24 July 2007
© Springer-Verlag 2007

Abstract We report concordant ages of 451.1 ± 6.0 and 450.5 ± 3.4 Ma from direct Rb–Sr and Re–Os isochron dating, respectively, of ore-stage Zn–Cu–Ge sulfides, including sphalerite for the giant carbonate-hosted Kipushi base metal (+Ge) deposit in the Neoproterozoic Lufilian Arc, DR Congo. This is the first example of a world-class sulfide deposit being directly dated by two independent isotopic methods. The 451 Ma age for Kipushi suggests that the ore-forming solutions did not evolve from metamorphogenic fluids mobilized syntectonically during the Pan-African-Lufilian orogeny but rather were generated in a Late Ordovician postorogenic, extensional setting. The homogeneous Pb isotopic composition of the sulfides indicates that both Cu–Ge- and Zn-rich orebodies of the Kipushi deposit formed contemporaneously from the same fluid system. The sulfide Pb isotope signatures in combination with initial $^{87}\text{Sr}/^{86}\text{Sr}$ and $^{187}\text{Os}/^{188}\text{Os}$ ratios defined by the isochrons point to metal sources located in the

(upper) crust. The concordant Re–Os and Rb–Sr ages obtained in this study provide independent proof of the geological significance of direct Rb–Sr dating of sphalerite.

Keywords Kipushi · Base metals · Copperbelt · Congo · Rb–Sr isotopes · Re–Os isotopes · Pb isotopes

Introduction

Precise constraints on the timing of mineralization are of fundamental importance in understanding the genesis of hydrothermal ore deposits. However, isotope geochronology of hydrothermal sulfide deposits has been proved problematic due to the lack of datable minerals in most of the common base metal mineralization types. Among the few isotopic methods applicable to hydrothermal base metal deposits, Rb–Sr and Re–Os dating of sulfides have attained increasing attractivity as these techniques allow for direct dating of common ore-forming minerals. The Re–Os chronometer, mostly utilized to date molybdenite (see Stein et al. 2001 and references therein), has been successfully applied to some common Cu–Fe sulfide minerals in a number of recent studies, including pyrite, chalcocite, and bornite (e.g., Stein et al. 2000; Morelli et al. 2004; Tristán-Aguilera et al. 2006). Like molybdenite, these sulfides may have extremely low concentrations of highly radiogenic Os, for which they have been termed LLHR (low-level, highly radiogenic) minerals by Stein et al. (2000). The pioneering work of Nakai et al. (1990) has demonstrated the suitability of sphalerite as a Rb–Sr geochronometer. Since then, the age of many carbonate-hosted base metal deposits has been successfully determined by direct Rb–Sr dating of sphalerite which has significantly advanced the genetic understanding of this mineralization style (see Christensen et al. 1996, and references therein).

Editorial handling: B. Lehmann

J. Schneider
Département de Minéralogie, Université de Genève,
Rue des Maraîchers 13,
1205 Geneva, Switzerland

F. Melcher
Bundesanstalt für Geowissenschaften und Rohstoffe,
Stilleweg 2,
30655 Hanover, Germany

M. Brauns
CEZ Archäometrie GmbH,
68159 Mannheim, Germany

J. Schneider (✉)
Geodynamics and Geofluids Research Group, Afdeling Geologie,
Katholieke Universiteit Leuven,
Celestijnenlaan 200E,
3001 Heverlee, Belgium
e-mail: Jens.Schneider@geo.kuleuven.be

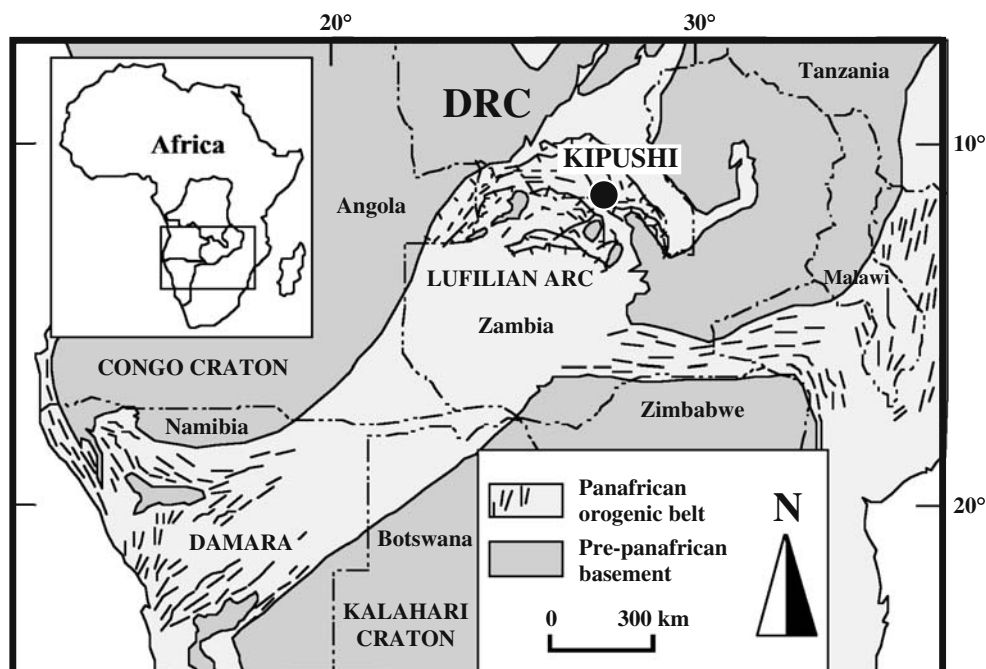
While most workers agree that the Re–Os chronometer provides robust ages for sulfide mineralization, it has been repeatedly suspected that the Rb–Sr system in sphalerite may be largely controlled by unrelated mineral inclusions such as micron-scale, detrital sheet silicates, thereby casting doubts on the reliability and geochronological significance of the method (e.g., Garven and Sverjensky 1994; Bradley and Leach 2003; Bradley et al. 2004). In this paper, we present a comparative geochronological study on the giant carbonate-hosted Kipushi base metal (+Ge) deposit, Democratic Republic of Congo (DRC), that employs direct Re–Os dating of Cu–Zn–Ge sulfides and Rb–Sr dating of sphalerite and bornite from discordant, epigenetic orebodies. Applying two different dating methods to sulfide ore minerals from the same deposit will provide internal, independent control on the isotopic ages so obtained, thereby contributing to a further critical evaluation of the Rb–Sr method applied to sphalerite. Complementary Pb isotope analyses of the dated sulfides will help to assess their paragenetic relationships.

Geology

The world-class Kipushi base metal deposit is located 30 km SW of Lubumbashi in southeastern DR Congo, at 27°14'E/11°47'S, within the northern extension of the Central African Copperbelt (Fig. 1). Kipushi is the largest among a number of Zn–Cu–Pb deposits in the Copperbelt. Its original ore reserves are estimated at >70 Mt at 8.8% Zn, 4.8% Cu, 0.5% Pb, 150 g/t Ag, and production between 1925 and 1993 amounted to ca. 60 Mt at 12% Zn, 8.0% Cu,

0.9% Pb (e.g., Höll et al. 2007). The geology and ore mineralization of the Kipushi deposit have been described in detail by De Vos et al. (1974), Intiomale and Oosterbosch (1974), and de Magnee and Francois (1988). The host rocks belong to the Katangan Supergroup, a Neoproterozoic, >9-km-thick succession in the foreland of the Pan-African–Lufilian Arc (Fig. 1) composed of dolomites, dolomitic shales, siltstones, sandstones, and arkoses. The Kipushi deposit is hosted in the upper Katangan Kundelungu Group (760–565 Ma; Key et al. 2001; Master et al. 2002) that consists of alternating carbonate rocks, shales, and sandstones and contains two diamictite horizons at the base of its lower and upper part, respectively. The orebodies at Kipushi occur at the northern margin of the Kipushi anticline along a steep, NNE striking fault zone (Kipushi Fault) at the contact between Kundelungu dolomites and dolomitic shales with a breccia body that occupies the core of the Kipushi anticline. The orebodies comprise a zone of stringer, massive, and semimassive sulfides about 600 m long and 15–75 m wide, striking in a north-easterly direction and dipping about 70° to the northwest. The sulfides occur in the fault plane, in joints, fractures, and bedding planes in the dolomite and as subvertical chimneys in carbonate rocks. The orebody has been traced from surface down to the 1,800-m level and it is open at depth. Zn–Cu–Pb sulfide mineralization is interpreted to be mostly epigenetic and forms (1) discordant bodies (Cu + Zn ca. 20%) filling cavities and voids in the collapse breccia and adjacent Kundelungu dolomites along the Kipushi Fault and (2) Zn-rich (up to 40%), elliptical pipe-like structures in massive, upper Kundelungu carbonate rocks. Broadly stratiform horizons of Cu-poor (ca. 2%) ores are confined

Fig. 1 Map of southern central Africa showing major geotectonic units and location of the Kipushi deposit (modified after Kamona et al. 1999)



to both sides of the boundary between the upper and lower Kundelungu Group. Sphalerite, Ag-bearing bornite, chalcocite, chalcopyrite, galena, and arsenopyrite are the principal ore minerals whereas a number of rare sulfosalts and sulfides including gallite and molybdenite occur in trace amounts. Abundant germanium sulfides such as renierite and briartite make the Kipushi deposit one of the largest known Ge anomaly in the Earth's crust; total past production amounted to ca. 120 t Ge (Höll et al. 2007).

Various contrasting models have been proposed for the genesis of the Kipushi deposit. Using structural criteria, Kampunzu et al. (1998) favored a synorogenic ore emplacement during D1 deformation in the Lufilian Arc (ca. 790–730 Ma) from tectonic brines and interpreted ore Pb isotope data from the literature to reflect binary mixing of distinct crustal Pb components ca. 750 Ma ago. Conversely, de Magneé and Francois (1988) suggested a postorogenic formation based on galena Pb–Pb model ages of ca. 425 Ma and by reference to U–Pb ages in the range of 525–500 Ma obtained for epigenetic uraninite from Copperbelt mineralizations. Walraven and Chabu (1994) and Kamona et al. (1999) interpreted galena Pb–Pb model ages of 454 ± 14 and 456 ± 18 Ma to reflect the age of mineralization at Kipushi, in agreement with U–Pb zircon ages in the range of 458–427 Ma for syenites located farther south. Kamona et al. (1999) suspected a significant mantle component in the Kipushi ore lead.

Samples and analytical methods

Two cores from drillholes 1270 and 787 that intersect Zn- and Cu–Ge-rich portions of the Kipushi deposit were sampled for this study. Sample types and drillhole depths are given in Tables 1 and 2. Drill core material was studied using reflected light microscopy, and the composition of sulfide phases was determined by electron microprobe (CAMECA SX 100) following procedures outlined in Melcher et al. (2006).

Germanium-rich sulfide ore from core 787 is mainly composed of renierite, chalcopyrite, and tennantite, subordinate bornite, sphalerite, briartite ($\text{Cu}_2(\text{Fe,Zn})\text{GeS}_4$), pyrite, arsenopyrite, galena, and traces of gallite (CuGaS_2), tungstenite, molybdenite, löllingite, and scheelite. Most conspicuous are exsolution intergrowth textures of Ga-bearing chalcopyrite (up to 18 wt.% Ga), gallite, and renierite in a number of samples (Fig. 2a,b). Renierite carries from 7 to 10 wt.% Ge, 2 to 3.5 wt.% Zn, and 13 to 15 wt.% Fe. Zinc-rich sulfide ore from core 1270 mainly consists of sphalerite and pyrite with partly abundant chalcopyrite, galena, arsenopyrite, and tennantite, and traces of stannite. A Cu-rich zone (Fig. 2c,d) carries Ag-rich bornite, chalcopyrite, sphalerite, tennantite, and accessory renierite and stromeyerite (CuAgS). Sphalerite has variable but low Fe concentrations, ranging from <1 to 6 wt.% Fe and from 0.4 to 0.6 wt.% Cd.

Table 1 Rb–Sr and Pb isotopic data of sphalerite and bornite samples from borehole 1270, Kipushi deposit

Sample	Depth ^a (m)	Mineral	Rb $\pm 2\sigma^b$ (ppb)	Sr $\pm 2\sigma^b$ (ppb)	$^{87}\text{Rb}/^{86}\text{Sr} \pm 2\sigma^b$	$^{87}\text{Sr}/^{86}\text{Sr} \pm 2\sigma^b$	$^{206}\text{Pb}/^{204}\text{Pb}$	$^{207}\text{Pb}/^{204}\text{Pb}$	$^{208}\text{Pb}/^{204}\text{Pb}$
KI 1270/ 113	R 108	sph	7.47 \pm 0.11	141.90 \pm 1.28	0.1524 \pm 0.0015	0.70994 \pm 0.00002	18.076	15.636	37.678
	L				0.1293 \pm 0.0016	0.71068 \pm 0.00002			
KI 1270/ 115	R 121	sph	14.33 \pm 0.10	117.30 \pm 0.84	0.3536 \pm 0.0037	0.71125 \pm 0.00003	18.018	15.635	37.666
	L				0.0293 \pm 0.0004	0.70991 \pm 0.00004			
KI 1270/ 122	R 136	bn	10.55 \pm 0.12	275.53 \pm 2.88	0.1052 \pm 0.0010	0.70965 \pm 0.00002	18.032	15.625	37.648
	L				0.0773 \pm 0.0010	0.70955 \pm 0.00001			
KI 1270/ 128	R 162	sph	1.89 \pm 0.02	8.84 \pm 0.09	0.6195 \pm 0.0067	0.71293 \pm 0.00002	18.008	15.634	37.692
	L				0.2456 \pm 0.0034	0.71143 \pm 0.00002			
KI 1270/ 135	R 197	sph	22.43 \pm 0.24	182.33 \pm 2.11	0.3560 \pm 0.0042	0.71129 \pm 0.00003	18.011	15.638	37.688
	L				0.0512 \pm 0.0007	0.71044 \pm 0.00003			

R Sphalerite/bornite residue; L corresponding fluid leachate; sph sphalerite; bn bornite

^a Refers to sampled borehole depth. ^b Absolute errors

Table 2 Re–Os and Pb isotopic data of renierite and bornite samples from borehole 787, Kipushi deposit

Sample	Depth ^a (m)	Mineral	Re±2σ ^b (ppb)	Os±2σ ^b (ppt)	¹⁸⁷ Re/ ¹⁸⁸ Os±2σ ^b	¹⁸⁷ Os/ ¹⁸⁸ Os±2σ ^b	²⁰⁶ Pb/ ²⁰⁴ Pb	²⁰⁷ Pb/ ²⁰⁴ Pb	²⁰⁸ Pb/ ²⁰⁴ Pb
KI 787/12	18.1	ren	17.98±0.18	87±1	29,820±417	224.00±1.12	18.017	15.630	37.667
KI 787/13	18.4	ren	49.36±0.49	256±3	28,127±394	211.68±1.06	18.038	15.637	37.711
KI 787/14	18.6	bn	17.66±0.18	118±1	2,255±32	16.60±0.08	17.989	15.646	37.775
KI 787/17	20.3	bn	36.49±0.37	207±2	4,450±62	32.84±0.16	17.987	15.640	37.734

ren Renierite; *bn* bornite

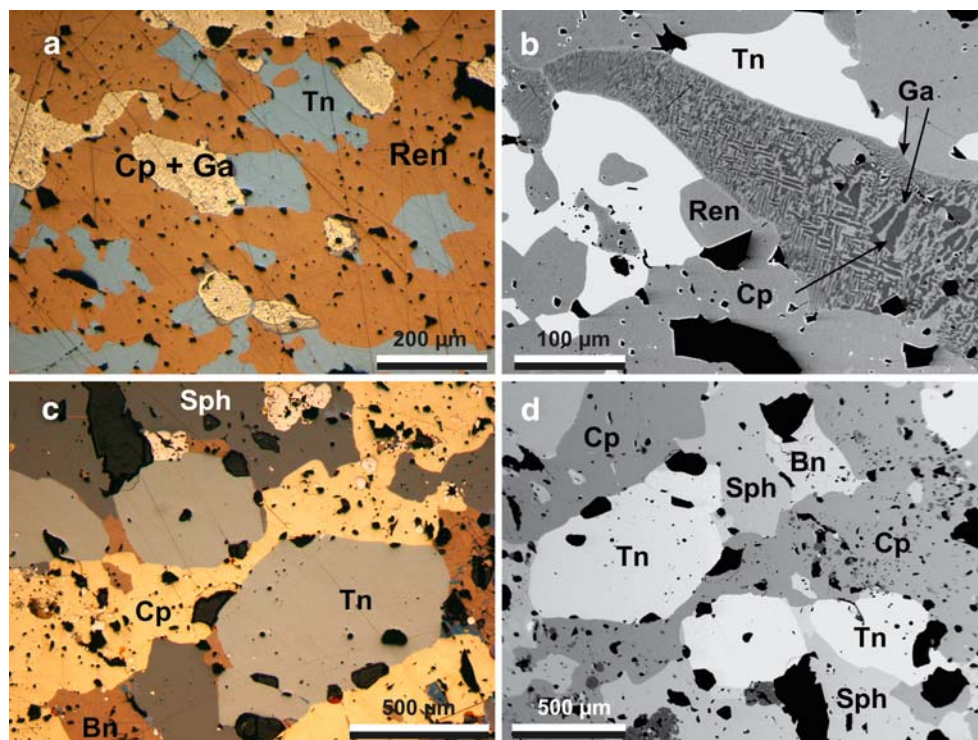
^a Refers to sampled borehole depth. ^b Absolute errors

All samples were carefully crushed, sieved (40–60 mesh-size fraction), and precleaned in deionized water. For Rb–Sr isotopic analysis, four sphalerite separates and one bornite sample were produced by careful handpicking of material extracted from core 1270, whereas the Re–Os work was performed on two separates of renierite (Cu₂₀Zn₂Ge₄Fe₈S₃₂) and two bornite samples obtained from core 787. Sphalerite and bornite separates for Rb–Sr dating and Pb isotope analysis were weighed and crushed in 400 µl of deionized water using a clean boron carbide mortar and pestle to extract and sample the inclusion fluids, following methods outlined in, e.g., Nelson et al. (2002). The fluid inclusion fractions were then separated from their sphalerite residuals by centrifuging and collected for separate Rb–Sr analysis. The crushed residues were subsequently leached with 2 N HCl for 10 min to remove possible unrelated carbonate contaminants and then repeatedly centrifuged and rinsed with deionized water until neutral reaction of the

supernate. The dry residues were then allowed to decompose in 2 ml of 6 N HCl (aqua regia for bornite) on a hot plate. Vial tops were lifted repeatedly to release H₂S. All sample solutions were totally spiked using a mixed tracer containing highly enriched ⁸⁷Rb and ⁸⁴Sr. Rubidium and strontium were separated with 3 N HNO₃ using EICHROM Sr resin on 50-µl Teflon columns. The first 600 µl of HNO₃ wash were collected for Rb and further purified using standard ion-exchange procedures. Sr was stripped from the columns with 1 ml of deionized water. Subsequently, Pb was eluted with 1 ml of 6 N HCl. The Pb cut was further processed through 50-µl columns containing precleaned EICHROM Pre Filter Resin.

The procedures for Re–Os isotopic analysis are fully described in Brauns (2001) and Woodhead and Brauns (2004). Renierite and bornite separates were weighed into Carius tubes prespiked with a mixed ¹⁸⁵Re–¹⁹⁰Os tracer and dissolved and equilibrated over 3 days using inverse aqua

Fig. 2 Reflected light (a, c) and electron back-scatter images (b, d) of Ge-rich sulphide ore (a, b) and Zn-rich sulphide ore (c, d) from Kipushi. *Bn*, bornite; *Cp*, chalcopyrite; *Ga*, gallite; *Ren*, renierite; *Sph*, sphalerite; *Tn*, tennantite



regia in an oven at ca. 240°C. Osmium as the volatile OsO_4 was then directly distilled from the Carius tubes, condensed on ca. 2 μl of chilled sulfuric acid and finally collected in 0.5 ml of 7 N HBr. Rhenium was recovered from the remaining solutions with 0.5–4 N HNO_3 on anion exchange columns using 1 ml AG1-X8 resin. Osmium was further purified using microdistillation techniques. Lead was separated from aliquots of the sample solutions used for the Re chemistry, following the procedure described above.

All isotopic measurements were performed on FINNI-GAN MAT 261/262 and THERMO ELECTRON TRITON thermal ionization mass spectrometers. Sr, Rb, Pb, and Re were measured in static multicollection mode on Faraday detectors using P-TIMS and N-TIMS methods, respectively, whereas Os isotope ratios were determined by N-TIMS using an ion-counting system. Details on mass spectrometry techniques and error propagation procedures are given in Schneider et al. (2003) and Woodhead and Brauns (2004). Total procedural blanks amounted to 10–25 pg Sr/2 pg Rb for sulfide residues, 20–50 pg Sr/5–12 pg Rb for the fluid leachates, 0.1 pg Os, and 5 pg Re. All data were blank-corrected, the uncertainties in $^{187}\text{Re}/^{188}\text{Os}$ and $^{187}\text{Os}/^{188}\text{Os}$ are conservatively estimated to be ± 1.3 – 1.4 and ± 0.5 %, respectively. Individual uncertainties (2σ) are given for Rb–Sr elemental concentrations and isotope ratios (Table 1).

Pb isotope ratios were corrected for instrumental mass fractionation using a mean discrimination factor of 0.085 ± 0.006 (2σ)/[amu], based on replicate measurements of the NBS SRM 981 common lead ($n=31$) standard. Errors and error correlations were calculated after Ludwig (1980); 2σ uncertainties for the corrected $^{206}\text{Pb}/^{204}\text{Pb}$, $^{207}\text{Pb}/^{204}\text{Pb}$, and $^{208}\text{Pb}/^{204}\text{Pb}$ ratios are ± 0.06 , 0.09 , and 0.12 %, respectively. The ISOPLOT/Ex version 3.00 software (Ludwig 2003) was used for Rb–Sr and Re–Os isochron regressions and errors on the ages are quoted at the 2σ level.

Results and discussion

The results of the Rb–Sr, Re–Os, and Pb–Pb isotopic analyses are given in Tables 1 and 2. The sulfide residues from drillcore 1270 have variable $^{87}\text{Rb}/^{86}\text{Sr}$ ratios between 0.10 and 0.62 and $^{87}\text{Sr}/^{86}\text{Sr}$ ratios ranging from 0.7099 to 0.7129. Their elemental concentrations (0.0019 to 0.0224 ppm Rb and 0.0088 to 0.2755 ppm Sr) are generally low and consistent with other published Rb–Sr data for sulfides (see Christensen et al. 1996 and references therein). Rb and Sr concentrations for the corresponding fluid leachates are not given, as the mass of fluids extracted during the crush-leach experiments cannot be determined with confidence. Re and Os abundances in bornite and renierite samples from drillcore 787 range from 17.6 to 49.4 and 87 to 256 ppt, respectively. The four samples have

$^{187}\text{Re}/^{188}\text{Os}$ ratios between 2,255 and 29,820 and show highly radiogenic $^{187}\text{Os}/^{188}\text{Os}$ ratios ranging from 32.8 to 224. In the absence of comparable literature data for renierite, our bornite samples have much higher Re–Os contents and $^{187}\text{Re}/^{188}\text{Os}$ ratios and higher radiogenic Os than those reported by Tristá-Aguilera et al. (2006) for bornite and chalcocite from a stratabound Cu deposit in northern Chile.

Both sulfide data sets define statistically well-supported Rb–Sr and Re–Os isochrons (MSWD=1.4 and 1.1) giving concordant Late Ordovician ages of 451.1 ± 6.0 and 450.5 ± 3.4 Ma, respectively, within errors (Fig. 3a,b). No linear data arrangement can be observed in the $^{87}\text{Sr}/^{86}\text{Sr}$ vs $1/\text{Sr}$ space (not shown), indicating that the line in Fig. 3a is not a pseudo-isochron produced by binary mixing of distinct Sr components. The initial $^{87}\text{Sr}/^{86}\text{Sr}$ ratio of the isochron (0.70897 ± 2) is slightly higher than published values for contemporaneous Late Ordovician seawater (Veizer et al. 1999) and reflects an overall crustal source for Sr. With exception of the bornite fluid leachate KI 1270/122 L, which plots close to its corresponding sulfide residue, all other leachates derived from sphalerite fall outside of the Rb–Sr sulfide isochron (Fig. 3a) indicating that they represent mixtures of primary and secondary fluid inclusions. This phenomenon has been observed in other datasets (Christensen et al. 1996 and references therein; Nelson et al. 2002) and makes the calculation of apparent leachate/sulfide residue pair ages insignificant. In Fig. 3b, the renierite samples show much higher Re–Os isotopic ratios than bornite. We attribute this systematic shift to specific yet unknown crystal chemical conditions that favor incorporation of Re into renierite rather than to contamination by micron-scale molybdenite, which forms a rare accessory phase at Kipushi. We would expect cogenetic and paragenetic bornite to be equally radiogenic if accessory molybdenite would control the Re–Os system in the Kipushi Cu–Ge sulfides which is, however, obviously not the case. The initial $^{187}\text{Os}/^{188}\text{Os}$ ratio of 0.74 ± 0.23 as defined by the Re–Os isochron in Fig. 3b is, despite its high uncertainty, much more radiogenic than the chondritic reference $^{187}\text{Os}/^{188}\text{Os}$ ratio of ca. 0.125 at 450 Ma. We infer that the Os contained in the Kipushi Cu–Ge sulfides is of crustal origin.

Figure 4 shows comparative Pb–Pb diagrams for all sulfides analyzed in this study and available data for galena samples from Kipushi (Walraven and Chabu 1994, Kamona et al. 1999). Sphalerite, bornite, and renierite display uniform Pb isotope signatures within errors, indicating that the Cu–Ge- and Zn-dominated portions of the Kipushi deposit are paragenetic and have formed contemporaneously from the same fluids. All samples plot close to the average crustal lead growth curve of Stacey and Kramers (1975). This indicates a crustal origin for lead, fully consistent with the crustal signatures of the Sr and Os

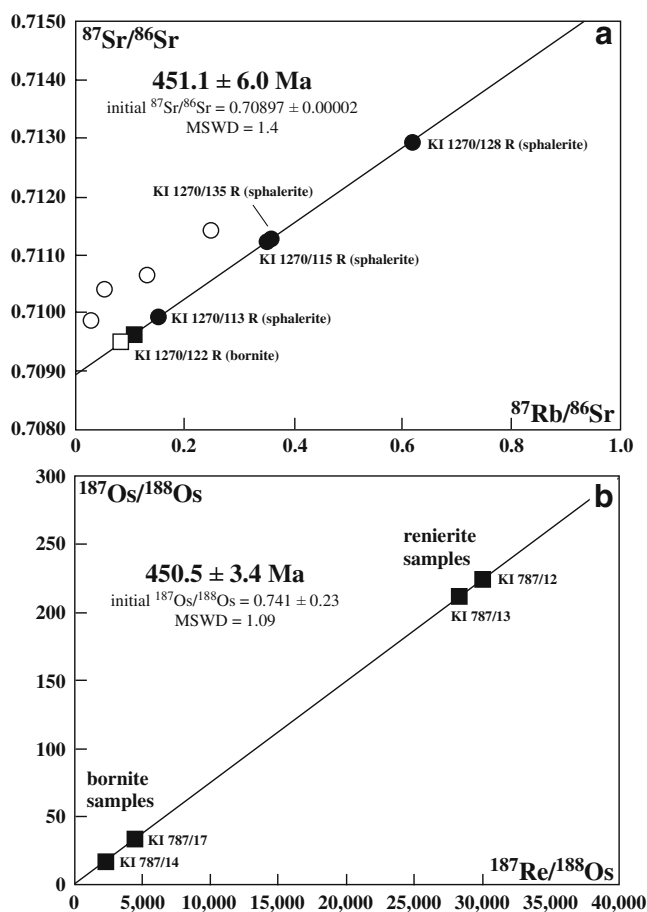


Fig. 3 Isotopic parent–daughter correlation diagrams for sulfide samples from Kipushi, **a** Rb–Sr data of four sphalerite residues (black dots), one bornite residue (black square), and corresponding fluid inclusion leachates (open circles, open square), **b** Re–Os data of two bornite and two renierite samples. All data from Tables 1 and 2. Isochron fits calculated using the ISOPLOT vs 3.00 routine of Ludwig (2003), $\lambda^{87}\text{Rb} = 1.42 \times 10^{-11} \text{ year}^{-1}$, $\lambda^{187}\text{Re} = 1.666 \times 10^{-11} \text{ year}^{-1}$

isochron initials in Fig. 3. The slightly enhanced $^{207}\text{Pb}/^{204}\text{Pb}$ and lowered $^{208}\text{Pb}/^{204}\text{Pb}$ ratios relative to the crustal average ratios point to upper crustal source rocks containing multistage lead components that partly evolved in ancient cratonic reservoirs. The Pb isotope population of our samples largely corresponds to the average of the depicted literature data. Therefore, we suspect that the linear trends observed in these data reflect instrumental mass fractionation rather than mixing of distinct Pb components as proposed by Kampunzu et al. (1998) and Kamona et al. (1999).

Conclusions

Ore-stage sulfides from an epigenetic base metal deposit have been dated directly by two independent isotopic methods for the first time, yielding concordant ages of 451 Ma for the world-class, carbonate-hosted Kipushi Zn–

Cu–Pb (+Ge) mineralization. This age is in agreement with previously published galena Pb–Pb model ages but much more precise and based on the analysis of complete parent/daughter isotope systems. The Rb–Sr and Re–Os ages truly represent mineralization ages as it is highly improbable that two geochemically distinct parent/daughter systems were reset simultaneously by any hypothetical postmineralization event, leaving little doubt in the reliability of both methods. Our combined Rb–Sr, Re–Os, and Pb–Pb study demonstrates that both Zn- and Cu–Ge-dominated orebodies at Kipushi formed from the same fluids during postorogenic extension in the Late Ordovician which refutes models of mineralization by tectonic brines during the Pan-African–Lufilian orogeny. Initial $^{87}\text{Sr}/^{86}\text{Sr}$ and $^{187}\text{Os}/^{188}\text{Os}$ ratios derived from Rb–Sr and Re–Os sulfide isochrons and Pb isotope data for the sulfides indicate crustal reservoirs as metal sources, ruling out a contribution from the mantle to the Kipushi orebodies.

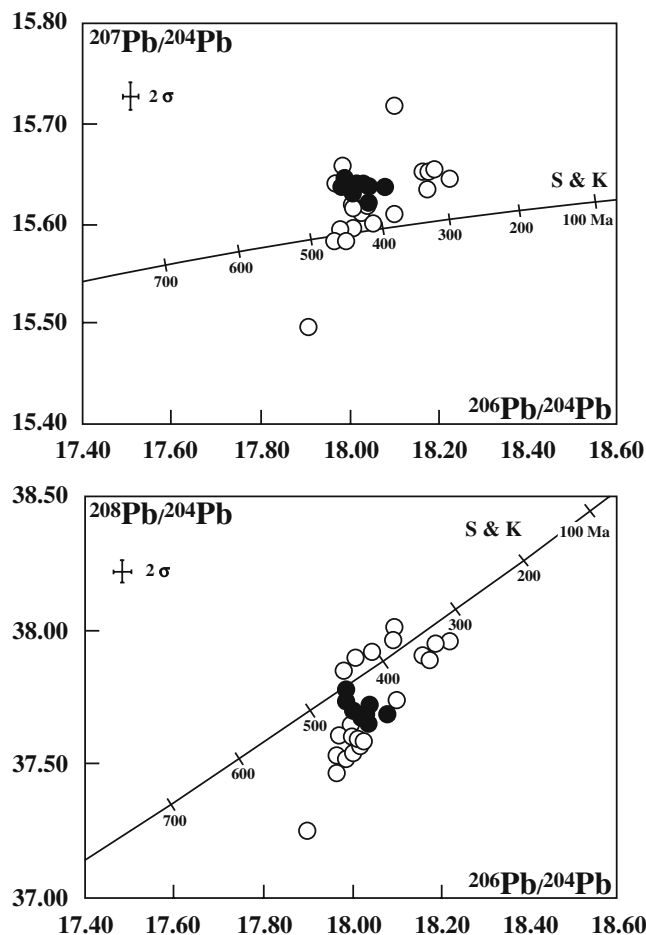


Fig. 4 Pb–Pb diagram showing all sulfides analyzed for Rb–Sr and Re–Os in this study (filled circles) and literature data for Kipushi galena (open circles, see text for references). S & K growth curve shown represents average crustal lead evolution after Stacey and Kramers (1975)

The concordant Re–Os and Rb–Sr ages obtained in this study provide independent proof of the geological significance of direct Rb–Sr dating of sphalerite. Likewise, Cu and Cu–Ge ores from carbonate-hosted base metal deposits appear suitable for Re–Os dating. Especially Ge sulfides show characteristics of typical LLHR sulfides, although the relative scarcity of Ge sulfides limits the wide applicability of Re–Os dating of such sulfides.

Acknowledgments This study was supported by Bundesanstalt für Geowissenschaften und Rohstoffe, 06035 Hannover, Germany. F.M. acknowledges the support and permission to sample drillcore material given by A. Kaputo Kalubi (Gecamines). We are grateful to S.E. Kesler, C.-T. Lee, and D. Selby for reviewing this paper.

References

- Bradley DC, Leach DL (2003) Tectonic controls of Mississippi Valley-type lead-zinc mineralization in orogenic forelands. *Miner Depos* 38:652–667
- Bradley DC, Leach DL, Symons D, Emsbo P, Premo W, Breit G, Sangster DF (2004) Reply to Discussion on “Tectonic controls of Mississippi Valley-type lead-zinc mineralization in orogenic forelands” by SE Kesler, JT Christensen, RD Hagni, W Heijlen, JR Kyle, KC Misra, P Muchez, R van der Voo. *Miner Depos* 39:515–519
- Brauns CM (2001) A rapid, low-blank technique for the extraction of osmium from geological samples. *Chem Geol* 176:379–384
- Christensen JN, Halliday AN, Kesler SE (1996) Radiometric dating of Mississippi Valley-type Pb–Zn deposits. In: Sangster DF (ed) Carbonate-hosted zinc–lead deposits. *Soc Econ Geol Spec Pub* 4:536–545
- de Magnée I, Francois A (1988) The origin of the Kipushi (Cu, Zn, Pb) deposit in direct relation with a Proterozoic salt diapir, Copperbelt of Central Africa, Shaba, Republic of Zaire. In: Friedrich GH, Herzig PM (eds) Base metal sulfide deposits in sedimentary and volcanic environments. Springer, New York, pp 74–93
- De Vos W, Viaene W, Moreau J, Wautier J (1974) Minéralogie du gisement de Kipushi Shaba Zaire. In: Bartholomé P (ed) Gisements stratiformes et provinces cuprifères. Centen Société Géol Belgique, Liège, pp 165–183
- Garven G, Sverjensky DA (1994) Paleohydrogeology of the Canadian Rockies and origins of brines Pb–Zn deposits and dolomitization in the Western Canada sedimentary basin: comment. *Geology* 22:1149–1150
- Höhl R, Kling M, Schroll E (2007) Metallogenesis of germanium—a review. *Ore Geol Rev* 30:145–180
- Intiomale M, Oosterbosch R (1974) Géologie et géochimie du gisement de Kipushi Zaire. In: Bartholomé P (ed) Gisements stratiformes et provinces cuprifères. Centen Société Géol Belgique, Liège, pp 123–164
- Kamona AF, Levque J, Friedrich G, Haack U (1999) Lead isotopes of the carbonate-hosted Kabwe, Tsumeb, and Kipushi Pb–Zn–Cu sulphide deposits in relation to Pan-African orogenesis in the Damaran–Lufilian fold belt of Central Africa. *Miner Depos* 34:273–283
- Kampunzu AB, Wendorff M, Kruger FJ, Intiomale MM (1998) Pb isotopic ages of sediment-hosted Pb–Zn mineralisation in the Neoproterozoic Copperbelt of Zambia and Democratic Republic of Congo (ex-Zaire): re-evaluation and implications. *Chron Rech Min* 530:55–61
- Key RM, Liyungu AK, Njamu FM, Somwe V, Banda J, Mosley PN, Armstrong RA (2001) The western arm of the Lufilian Arc in NW Zambia and its potential for copper mineralization. *J Afr Earth Sci* 33:503–528
- Ludwig KR (1980) Calculation of uncertainties of U–Pb isotope data. *Earth Planet Sci Lett* 46:212–220
- Ludwig KR (2003) Isoplot/Ex version 300 A geochronological toolkit for Microsoft Excel. Berkeley Geochron Center Spec Pub 4:1–43
- Master S, Rainaud C, Armstrong RA, Phillips D, Robb LJ (2002) Contributions to the geology and mineralisation of the central African Copperbelt: II Neoproterozoic deposition of the Katanga Supergroup with implications for regional and global correlations. 11th IAGOD Quadr Symposium and Geocongress 2002, 22–26 July 2002, Windhoek Namibia. Ext Abstr (CD-ROM)
- Melcher F, Oberthür T, Rammlmair D (2006) Geochemical and mineralogical distribution of germanium in the Khusib Springs Cu–Zn–Pb–Ag sulfide deposit Otavi Mountain Land, Namibia. *Ore Geol Rev* 28:32–56
- Morelli RM, Creaser RA, Selby D, Kelley KD, Leach DL, King AR (2004) Re–Os sulfide geochronology of the Red Dog sediment-hosted Zn–Pb–Ag deposit, Brooks Range, Alaska. *Econ Geol* 99:1569–1576
- Nakai S, Halliday AN, Kesler SE, Jones HD (1990) Rb–Sr dating of sphalerites from Tennessee and the genesis of Mississippi Valley type ore deposits. *Nature* 346:354–357
- Nelson J, Paradis S, Christensen J, Gabites J (2002) Canadian Cordilleran Mississippi Valley-type deposits: A case for Devonian–Mississippian back-arc hydrothermal origin. *Econ Geol* 97:1013–1036
- Schneider J, Haack U, Stedingk K (2003) Rb–Sr dating of epithermal vein mineralization stages in the eastern Harz Mts (Germany) by paleomixing lines. *Geochim Cosmochim Acta* 67:1803–1819
- Stacey JS, Kramers JD (1975) Approximation of terrestrial lead isotope evolution by a two-stage model. *Earth Planet Sci Lett* 26:207–221
- Stein HJ, Morgan JW, Scherstén A (2000) Re–Os dating of low-level highly radiogenic (LLHR) sulfides: The Harnäs gold deposit, southwest Sweden, records continental-scale tectonic events. *Econ Geol* 95:1657–1671
- Stein HJ, Markey RJ, Morgan JW, Hannah JL, Scherstén A (2001) The remarkable Re–Os chronometer in molybdenite: how and why it works. *Terra Nova* 13:479–486
- Tristá-Aguilera D, Barra F, Ruiz J, Morata D, Talavera-Mendoza O, Kojima S, Ferraris F (2006) Re–Os isotope systematics for the Lince–Estefanía deposit: constraints on the timing and source of copper mineralization in a stratabound copper deposit, Coastal Cordillera of Northern Chile. *Miner Depos* 41:99–105
- Veizer J, Ala D, Azmy K, Bruckschen P, Bruhn F, Buhl D, Carden G, Diener A, Ebner S, Goddard Y, Jasper T, Korte C, Pawellek F, Podlaha O, Strauss H (1999) $^{87}\text{Sr}/^{86}\text{Sr}$, $\delta^{18}\text{O}$ and $\delta^{13}\text{C}$ evolution of Phanerozoic seawater. *Chem Geol* 161:59–88
- Walraven F, Chabu M (1994) Pb-isotopic constraints on base metal mineralisation at Kipushi (Southeastern Zaire). *J Afr Earth Sci* 18:73–82
- Woodhead J, Brauns M (2004) Current limitations to the understanding of Re–Os behaviour in subduction systems, with an example from New Britain. *Earth Planet Sci Lett* 221:309–323